

**Continental Scale Comparisons of Terrestrial Carbon Sinks  
Estimated from Satellite Data and Ecosystem Modeling 1982-1998**

Christopher Potter <sup>1\*</sup>, Steven Klooster <sup>2</sup>, Ranga Myneni <sup>3</sup>,  
Vanessa Genovese <sup>2</sup>, Pang-Ning Tan <sup>4</sup>, Vipin Kumar <sup>4</sup>,

<sup>1</sup> NASA Ames Research Center, Moffett Field, CA

<sup>2</sup> California State University Monterey Bay, Seaside, CA

<sup>3</sup> Boston University, Boston, MA

<sup>4</sup> University of Minnesota, Minneapolis, MN

Please return comments and other correspondence to:

\* Corresponding author at

Email: [cpotter@gaia.arc.nasa.gov](mailto:cpotter@gaia.arc.nasa.gov)

Tel. 650-604-6164; Fax. 650-604-4680

Revised Draft Date: January 14, 2003

Submission to: *Global and Planetary Change*

**Abstract.** A simulation model based on satellite observations of monthly vegetation cover was used to estimate monthly carbon fluxes in terrestrial ecosystems from 1982 to 1998. The NASA-CASA model was driven by vegetation properties derived from the Advanced Very High Resolution Radiometer and radiative transfer algorithms that were developed for the Moderate Resolution Imaging Spectroradiometer (MODIS). For the terrestrial biosphere, predicted net ecosystem production (NEP) flux for atmospheric CO<sub>2</sub> has varied widely between an annual source of -0.9 Pg C per year and a sink of +2.1 Pg C per year. The southern hemisphere tropical zones (SHT, between 0° and 30° S) have a major influence over the predicted global trends in interannual variability of NEP. In contrast, the terrestrial NEP sink for atmospheric CO<sub>2</sub> on the North American (NA) continent has been fairly consistent at between +0.2 and +0.3 Pg C per year, except during relatively cool annual periods when continental NEP fluxes are predicted to total to nearly zero. The predicted NEP sink for atmospheric CO<sub>2</sub> over Eurasia (EA) increased notably in the late 1980s and has been fairly consistent at between +0.3 and +0.55 Pg C per year since 1988. High correlations can be detected between the El Niño-Southern Oscillation (ENSO) and predicted NEP fluxes on the EA continent and for the SHT latitude zones, whereas NEP fluxes for the North American continent as a whole do not correlate strongly with ENSO events over the same time series since 1982. These observations support the hypothesis that regional climate warming has had notable but relatively small-scale impacts on high latitude ecosystem (tundra and boreal) sinks for atmospheric CO<sub>2</sub>.

Key Words: carbon dioxide, ecosystems, remote sensing, ocean climate

## 1. Introduction

Less than 50% of the carbon emitted to the atmosphere each year through forest loss, fossil fuel combustion, and industrial activities remains in the atmosphere. The remainder of the carbon emitted through these human activities is reabsorbed and stored as sinks, perhaps temporarily, in the oceans and in terrestrial ecosystems (Schimel et al., 2001). This is the so-called "missing sink" for carbon dioxide emissions. Measured atmospheric CO<sub>2</sub>, <sup>13</sup>C, and O<sub>2</sub>/N<sub>2</sub> distributions indicate that during the past two decades a large fraction of the missing carbon sink has been on land (Bender et al., 1996; Keeling et al., 1996; Rayner et al., 1999), specifically in the temperate and boreal latitudes of the Northern Hemisphere. Nevertheless, the mechanisms and the precise spatial pattern of a sink for CO<sub>2</sub> in the terrestrial biosphere remain uncertain, to a large degree because the heterogeneity of land cover and ecosystem exchange processes have not been measured in adequate detail to determine precise regional sink contributions for atmospheric CO<sub>2</sub> (USGCRP, 1999; Watson et al., 2000).

Uncertainties in terrestrial carbon fluxes may be reduced with the development of improved modeling techniques for estimating variability in ecosystem processes over vast land areas (IGBP, 1998). Global ecosystem models (e.g., Maisongrande et al. 1995; Kindermann et al., 1996; McGuire et al., 2001) are valuable tools in situations when ground-based measurements of carbon fluxes are not adequate to realistically capture variability on a regional basis. A computer model of this type based on satellite measurements of vegetation cover has been developed to simulate global ecosystem carbon cycling (Potter and Klooster, 1997 and 1998; Potter 1999). Our NASA-CASA (Carnegie Ames Stanford Approach) model is designed

to estimate monthly patterns in carbon fixation, plant biomass, nutrient allocation, litter fall, soil nutrient mineralization, and CO<sub>2</sub> exchange, including carbon emissions from soils world-wide.

Direct input of satellite “greenness” data from the Advanced Very High Resolution Radiometer (AVHRR) sensor into the NASA-CASA model are used to estimate spatial variability in monthly net primary production (NPP), biomass accumulation, and litter fall inputs to soil carbon pools at a geographic resolution of 0.5° latitude/longitude. Global NPP of vegetation is predicted using the relationship between greenness reflectance properties and the fraction of absorption of photosynthetically active radiation (FPAR), assuming that net conversion efficiencies of PAR to plant carbon can be approximated for different ecosystems or are nearly constant across all ecosystems (Sellers et al., 1984; Running and Nemani, 1988; Goetz and Prince, 1998). In this study, we compare the results of NASA-CASA model predictions from 1982 to 1998 to infer variability in continental scale carbon fluxes and to understand global climate control patterns over terrestrial carbon sinks.

## **2. Modeling Methods and Global Drivers**

As documented in Potter (1999), the monthly NPP flux, defined as net fixation of CO<sub>2</sub> by vegetation, is computed in NASA-CASA on the basis of light-use efficiency (Monteith, 1972). Monthly production of plant biomass is estimated as a product of time-varying surface solar irradiance,  $S_r$ , and FPAR from the satellite AVHRR, plus a constant light utilization efficiency term ( $e_{max}$ ) that is modified by time-varying stress scalar terms for temperature (T) and moisture (W) effects (Equation 1).

$$\text{NPP} = S_r \text{ FPAR } e_{\text{max}} T W \quad (1)$$

The  $e_{\text{max}}$  term is set uniformly at  $0.39 \text{ g C MJ}^{-1} \text{ PAR}$ , a value that derives from calibration of predicted annual NPP to previous field estimates (Potter et al., 1993). This model calibration has been validated globally by comparing predicted annual NPP to more than 1900 field measurements of NPP (Figure 1). Interannual NPP fluxes from the CASA model have been reported (Behrenfeld et al., 2001) and validated against multi-year estimates of NPP from field stations and tree rings (Malmström et al., 1997).

The T stress scalar is computed with reference to derivation of optimal temperatures ( $T_{\text{opt}}$ ) for plant production. The  $T_{\text{opt}}$  setting will vary by latitude and longitude, ranging from near  $0^{\circ}\text{C}$  in the Arctic to the middle thirties in low latitude deserts. The W stress scalar is estimated from monthly water deficits, based on a comparison of moisture supply (precipitation and stored soil water) to potential evapotranspiration (PET) demand using the method of Priestly and Taylor (1972).

Evapotranspiration is connected to water content in the soil profile layers (Figure 2), as estimated using the NASA-CASA algorithms described by Potter (1999). The soil model design includes three-layer ( $M_1$ - $M_3$ ) heat and moisture content computations: surface organic matter, topsoil (0.3 m), and subsoil to rooting depth (1 to 2 m). These layers can differ in soil texture, moisture holding capacity, and carbon-nitrogen dynamics. Water balance in the soil is modeled as the difference between precipitation or volumetric percolation inputs, monthly estimates of PET, and the drainage output for each layer. Inputs from rainfall can recharge the soil layers to

field capacity. Excess water percolates through to lower layers and may eventually leave the system as seepage and runoff. Freeze-thaw dynamics with soil depth operate according to the empirical degree-day accumulation method (Jumikis, 1966), as described by Bonan (1989).

Based on plant production as the primary carbon and nitrogen cycling source, the NASA-CASA model is designed to couple daily and seasonal patterns in soil nutrient mineralization and soil heterotrophic respiration ( $R_h$ ) of  $CO_2$  from soils worldwide. Net ecosystem production (NEP) can be computed as NPP minus  $R_h$  fluxes, excluding the effects of small-scale fires and other localized disturbances or vegetation regrowth patterns on carbon fluxes (Walker and Steffen, 1997). The NASA-CASA soil model uses a set of compartmental difference equations with a structure comparable to the CENTURY ecosystem model (Parton et al., 1992). First-order decay equations simulate exchanges of decomposing plant residue (metabolic and structural fractions) at the soil surface. The model also simulates surface soil organic matter (SOM) fractions that presumably vary in age and chemical composition. Turnover of active (microbial biomass and labile substrates), slow (chemically protected), and passive (physically protected) fractions of the SOM are represented. Along with moisture availability and litter quality, the predicted soil temperature in the M1 layer controls SOM decomposition. Soil fertility factors are included in the NASA-CASA model, which control the allocation of new plant growth to above ground tissues (leaf and wood) versus fine root tissue allocation for acquisition of soil nutrients (Potter, 1999).

Whereas previous versions of the NASA-CASA model (Potter et al., 1993 and 1999) used a normalized difference vegetation index (NDVI) to estimate FPAR, the current model

version instead relies upon canopy radiative transfer algorithms (Knyazikhin et al., 1998), which are designed to generate improved FPAR products as inputs to carbon flux calculations. These radiative transfer algorithms, developed for the MODIS (Moderate Resolution Imaging Spectroradiometer) instrument aboard the NASA Terra platform, account for attenuation of direct and diffuse incident radiation by solving a three-dimensional formulation of the radiative transfer process in vegetation canopies. Monthly composite data from channels 1 and 2 of the AVHRR have been processed according to the MODIS radiative transfer algorithms and aggregated over the global land surface to 0.5° resolution, consistent with the NASA-CASA climate driver data. To minimize cloud contamination effects, a maximum value composite algorithm was applied spatially for 0.5 degree pixel values.

Gridded climate drivers of mean monthly solar radiation, air surface temperature (TEMP), and precipitation (PREC) come from interpolated weather station records (New et al., 2000) distributed across all the continental masses. Land cover categories for vegetation types are derived from AVHRR classification products (DeFries et al., 1995).

The NASA-CASA soil carbon pools were initialized to represent storage and flux conditions in near steady state (annual NEP less than 0.5% of global annual NPP) with respect to mean land surface climate recorded for the period 1979-1981 (New et al., 2000). This initialization protocol was found to be necessary to eliminate any notable discontinuities in predicted NEP fluxes during the transition to our model simulation years of interest, which were run on a monthly time step starting January 1982 to December 1998 using interannual FPAR and climate drivers. When this soil carbon initialization step is not properly included, we note that

an ecosystem model will likely predict artificially large carbon sinks in the terrestrial biosphere that then diminish as an artifact feature over the actual simulation period of interest as the model eventually approaches steady state. Initializing to near steady state does not, however, address the issue that some ecosystems are not in equilibrium with respect to net annual carbon fluxes, especially when they are recovering from past disturbances. Therefore, the most appropriate initialization would be to prescribe observed soil carbon pools, for which we do not have enough global data. Thus, although initialization to near steady state is common practice, it is also an assumption in the modeling method.

Accumulation of carbon in due to changes in plant biomass have been reported in a previous paper by Potter (1999) using the NASA-CASA model. Predicted aboveground biomass (AGB; including leaf and wood C) was estimated at 651 Pg C for the globe. Average carbon storage in AGB was predicted to be highest in broadleaf evergreen forests, mostly in the tropical zones, at more than 12 kg C m<sup>-2</sup>, followed by mixed coniferous-deciduous forests of the temperate zones. Net terrestrial losses of CO<sub>2</sub> from changes in the world's forest ecosystems are between 1.2-1.3 Pg C yr<sup>-1</sup> for the early 1990s. This estimate includes areas of forest regrowth and expansion as carbon sinks in temperate and boreal forest zones based on the recent global maps for observed climate, soils, plant cover, and changes in forest areas from natural and human forces.

### **3. Model Results for Terrestrial Carbon Fluxes**

For comparison purposes, we define the continental areas for both North America (NA) and Eurasia (EA) as latitude zones higher than 13.5° N within their respective western and eastern sides of the Atlantic ocean. The southern hemisphere tropical (SHT) zone is defined as the latitudes between the equator and 30° S across the entire globe. In terms of predicted NPP for these areas, the NA continent was estimated to vary between 6 and 7.5 Pg C per year (1 Pg =  $10^{15}$  g), the EA continent was estimated to vary between 11 and 13 Pg C per year, and the SHT zone was estimated to vary between 16 and 18.5 Pg C per year. Global terrestrial NPP was estimated to vary between 45 and 51 Pg C per year. These results for regional NPP fluxes are all consistent with those reported by Schimel et al. (2001) based largely on predictions from numerous other global ecosystem models and inventories. As further noted by Schimel et al. (2001), the larger NPP fluxes predicted by our model for EA compared to NA are mainly a function of larger total land area coverage over the EA region, rather than higher per unit area NPP fluxes over most of the continents.

Continental and global scale NEP results from NASA-CASA interannual simulations imply the following patterns in ecosystem carbon fluxes:

- (a) Since 1982, the terrestrial NEP sink for atmospheric CO<sub>2</sub> in NA has been fairly consistent at between +0.2 and +0.3 Pg C per year, except during relatively cool yearly periods like 1987, 1991-92, and 1995-96 when the NA continental NEP is predicted to be close to zero net flux of CO<sub>2</sub> (Figure 3).
- (b) The terrestrial NEP sink for atmospheric CO<sub>2</sub> in EA increased notably in the late 1980s and has been fairly consistent at between +0.3 and +0.55 Pg C per year since 1988, except

- during relatively cool periods like 1991-92 and 1995-96 when the EA continental NEP sink is predicted to vary between +0.1 and +0.25 Pg C per year (Figure 4).
- (c) The global NEP flux for atmospheric CO<sub>2</sub> has varied between an annual source of -0.9 Pg C per year to a sink of +2.1 Pg C per year (Figure 5), with the SHT zones having a major influence over global interannual variability (at between -0.3 and +0.8 Pg C per year).
  - (d) The global NEP flux for CO<sub>2</sub> has tended to increase from negative (net source flux to the atmosphere) in the early 1980s to a consistently positive (net sink flux from the atmosphere) by the mid to late 1990s.

Estimates of net annual carbon sinks for NA reported in this study fall well within the range estimated for continental carbon fluxes assembled by Pacala et al. (2001) and Houghton et al. (1999), mainly from land-based studies. At the global level, comparison of terrestrial NEP flux predictions from NASA-CASA to inverse model estimates for net exchange of atmospheric CO<sub>2</sub> with the terrestrial biosphere (Bousquet et al., 2000) indicate a close agreement from 1982-1990 between the two independent methods for estimating net carbon flux on land (Figure 5). For the period 1991-1995, however, the two modeling predictions diverge markedly, with the NASA-CASA model initially predicting a moderate source flux of CO<sub>2</sub> to the atmosphere followed by a larger sustained sink flux during 1993-1995, and the inverse model predicting essentially the reverse trend. It should be noted that the inverse model estimate can include sources of terrestrial carbon emitted to the atmosphere from ecosystem disturbances, such as wild fires, whereas the NASA-CASA model does not include these additional source fluxes of CO<sub>2</sub>. Consequently, because the two models predict somewhat different sub-components of the global carbon cycle, it is possible that both model predictions could be reasonably correct

representations of actual fluxes during periods when NASA-CASA predicts a net terrestrial sink for atmospheric CO<sub>2</sub>, but the inverse model predicts an additional source flux.

Although our ecosystem modeling results show several consecutive multi-year periods during which the magnitudes of continental sinks for CO<sub>2</sub> were fairly constant, the predicted spatial pattern of these sink fluxes can be highly variable. An example of this result is shown for NA during the years 1996 to 1998 (Figure 6). All three years are predicted to have continental NEP sink fluxes of 0.1-0.3 Pg C, but the spatial distribution of the annual carbon sink is quite different in each of three years. For example, during 1996, a year not marked by substantial regional warming (compared to 1995) nor by above-average precipitation on a continental scale (Figure 7), the predicted continental sink for carbon is localized mainly along the eastern portions of the United States and southern Canada. In 1997, substantial regional warming and above-average precipitation were observed, leading to a shift in the major sink areas on the continent to northwestern Canada and portions of the central United States. In 1998, a year closely matching 1997 in total NEP flux of about +0.2 Pg C for NA, regional warming continued and above-average precipitation was observed, leading to another shift in the major sink areas on the continent to southeastern portions of Canada and the United States. These variable spatial patterns of annual carbon sinks within a continental area, which are nearly the same in total flux magnitude, can be investigated in greater detail by examining impacts of large scale climate dynamics, like El Niño events and global teleconnections, on the model's climate controller variables (TEMP and PREC) for terrestrial NPP and NEP on regional scales.

## **4. Understanding Global Climate Controls on Ecosystem Production**

Our NASA-CASA model results are consistent with the findings of McGuire et al. (2001), Vukicevic et al. (2001), and Braswell et al. (1997) that, globally, there appears to be a net release of carbon to the atmosphere during warm and dry El Niño years, and a net uptake during cooler and wetter non El Niño years. However, our results suggest that this climate control pattern applies mainly to the tropical zones of the terrestrial biosphere. Relatively cool periods in the northern zones (30°-60° N) are not commonly associated with net carbon sinks. Vukicevic et al. (2001) postulated that climate warming should increase NPP in northern ecosystems, but that soil  $R_h$  should increase more than NPP, leading to decreased or negative NEP. Results from our NASA-CASA model do not strongly support this hypothesis. We find instead that surface warming on the NA and EA continents has increased observed FPAR and predicted NPP during the 1990s at rates that have exceeded subsequent  $R_h$  losses from decomposition. This could result, at least partially, because litterfall (particularly from needleleaf trees), the most labile substrate for decomposition, and responses of soil  $R_h$  to climate, which lag high seasonal NPP fluxes long enough to desynchronize these component fluxes of NEP over time.

### **4.1 Association Analysis for NPP and NEP Controllers**

Association rule analysis can offer useful insights into the types of dependencies that exist among variables within a large data set. Non-random associations between two or more model variables are reported here using the chi-square test (Stockburger 1998). Chi-square values greater than 3.84 (degrees of freedom=1) indicate a high probability ( $p < 0.05$ ) of non-random association between anomalously low (LO) or anomalously high (HI) monthly events for

TEMP, PREC, or  $S_T$  (solar irradiance) with either NPP or NEP. We used an anomalous event threshold value of 1.5 standard deviations or greater from the long-term (1982-1998) monthly mean value. For our analysis, association patterns are reported below on the basis of frequency of occurrence within major global vegetation types (DeFries et al., 1995).

We find that one of the strongest non-random associations in our NASA-CASA results is that PREC-LO events co-occur with NPP-LO and with NEP-LO events in evergreen broadleaf forests, deciduous broadleaf forests, croplands, and grassland savannas (Figure 8a). These events occur mainly in drought-sensitive areas of tropical and sub-tropical zones, and possibly in areas of major wild fires that are associated with FPAR-LO events. We also find that TEMP-HI events co-occur with NPP-LO events for these same vegetation types, which can be another indicator of drought stress effects on plant carbon gains.

Another non-random association rule indicates that TEMP-HI events co-occur with NPP-HI and NEP-HI events in tundra, grasslands, deciduous needleleaf forests, evergreen needleleaf forests, and mixed (needleleaf-broadleaf) forests (Figure 8b), even with co-occurring PREC-LO events. These observations lead to the hypothesis that regional climate warming has had the greatest impact on high latitude (tundra and boreal) sinks for atmospheric  $CO_2$ , particularly over the EA continent.

We find in addition that PREC-HI plus TEMP-HI events co-occur with NPP-HI and NEP-HI events in mixed forests, deciduous broadleaf forests, and evergreen needleleaf forests. This non-random association suggests an important dual control over net carbon fluxes by PREC

and TEMP events in transition zones between cool temperate and warmer sub-tropical forest ecosystems.

#### **4.2 Correlations with Climate Indices**

The influence of ocean surface climate events, such as the El Niño-Southern Oscillation (ENSO), on atmospheric circulation and land surface climate have been noted as a significant global teleconnection (Glantz et al., 1991). Teleconnection is a term used in meteorological studies to describe simultaneous variation in climate and related processes over widely separated points on earth. There are different phases in climate indices (CIs) such as the ENSO, which is called El Niño in the warm phase and La Niña in the cold phase. ENSO warming at the sea surface, which is driven by changes in winds and ocean-atmosphere heat exchange, typically extends to about 30°N and 30°S latitude, with lags into continental land areas of several months. The Southern Oscillation Index (SOI) is an indicator of atmospheric impacts of ENSO, computed as the standardized difference between sea level pressure (SLP) measured in Tahiti (17°S, 149°W) and Darwin, Australia (13°S, 131°E).

The SOI is commonly used to document warm-phases in ENSO, which are often associated with above-average temperatures in the northwestern half of the North American continent, and below-average temperatures in the southeastern half (Trenberth and Hurrell, 1994; Klein et al., 1999; McCabe and Dettinger, 1999). There is also a pattern of the warm-phase ENSO associated with above-average precipitation over western coastal South America (Vuille et al., 2000), the southern United States and northern Mexico, plus below-average precipitation

in south-central Africa, northeastern South America, parts of southern Asia and Australia, and in North America from the Canadian Rockies to the Great Lakes region.

In contrast to ENSO, the North Atlantic Oscillation (NAO) index refers to the north-south oscillation in atmospheric mass between the Icelandic low (65°N, 22°W) and the Azores high pressure centers from 39°N, 9°W to 36°N, 6°W (Walker and Bliss, 1932; Thompson and Wallace, 1998). The atmospheric state indexed by negative NAO corresponds to a southward displacement of winter storms and moisture transport across the North Atlantic into southern Europe (Hurrell 1995). A positive NAO corresponds to northward displacement of storms and moisture in northernmost Europe and Russia. During winter months when the NAO index is high, anomalously low precipitation commonly occurs over the Canadian Arctic, central and southern Europe, the Mediterranean and Middle East. Conversely, anomalously high precipitation occurs from Iceland though Scandinavia. In the eastern United States, winters with negative NAO are characterized by more northerly winds, which reduce moisture transports into the region from the south. The NAO can also represent the persistence of below-average temperature variations over North Africa and the Middle East, and above-average temperatures over North America (Hurrell, 1995).

Using matching monthly records for the period of 1982-1998, significant relationships between the time series anomalies of SOI or NAO and carbon (NPP or NEP) fluxes from our NASA-CASA model were identified using Pearson's correlation coefficient ( $r$ ). In each of these comparison cases, serial correlation (i.e., autocorrelation) needs to be considered when testing significance of the relationship between two time series. Hence, we first determined the serial

correlation of CIs at all possible lag times. SOI anomalies have a low autocorrelation function ( $< 0.3$ ) at lag times greater than about 6 months (using index data from 1958-1995). For NAO anomalies, the autocorrelation function is  $< 0.1$  at lag times greater than 3 months. For our predicted NPP anomalies, the autocorrelation function is  $< 0.1$  at lag times greater than 6 months. Based on these results, we accepted degrees of freedom (df) for the CI time series correlations with NPP and NEP fluxes to be  $df=32$  (34 'seasons' of 6 months duration in a 17-year window, minus 2 for a 2-tailed test of significance).

The highest correlations were detected between the deseasonalized time series for SOI with global terrestrial NEP at  $r=0.43$  ( $p<0.05$  with 3 mo lag; Figure 5), for SOI with SHT NEP at  $r=0.44$  ( $p <0.05$  with 6 mo lag), and for SOI with EA NEP at  $r=0.34$  ( $p <0.05$  with 3 mo lag). In contrast, all global and continental scale correlations between SOI and NPP were found to be low ( $r <0.2$ ), a pattern also reported by Behrenfeld et al. (2001) using the CASA NPP model, albeit for a much short period of 1997-2000. We also found low correlation between SOI and NA NEP ( $r <0.25$ ) for 1982-1998. This is not to imply that there were no high correlations between SOI and NPP or NEP time series for many sub-continental areas. On the contrary, on small scales, predicted NPP fluxes from the NASA-CASA model can be highly correlated with SOI, particularly for areas of the southern United States, northeastern South America, south-central Africa, and parts of southern Asia and Australia.

We could detect no high correlations ( $r >0.3$ ) between the deseasonalized time series for NAO index with NPP or NEP at either global or continental scales. These results support the hypothesis that the NAO has relatively small-scale effects on interannual variations in land

surface climate and terrestrial carbon fluxes, at least compared to ENSO. Areas over northern Canada and the EA continent represent prime examples of these small-scale effects of NAO on predicted NPP from the model.

As implied in the previous section, deseasonalized time series for NPP and NEP fluxes for the entire NA continent were positively correlated with continental TEMP anomalies (Figure 7), at  $r=0.49$  NPP and at  $r=0.39$  NEP ( $p < 0.05$ ), although not significantly correlated with continental PREC anomalies. Over the same period, continental scale correlations between SOI or NAO and mean TEMP anomalies were found to be low ( $r < 0.15$ ), whereas the correlation between SOI and continental PREC anomalies was significant ( $r = -0.43$ ;  $p < 0.05$ ). This series of results suggest that teleconnections of commonly used climate indices like SOI and NAO to terrestrial carbon cycles of NA develop as relatively small-scale and temporally varying combinations of climate controls. It also implies that the regional climate warming and high latitude (tundra and boreal) sinks for atmospheric CO<sub>2</sub> predicted over NA during the 1990s are not strongly ENSO-related.

The relative impacts of PREC, TEMP, and FPAR time series inputs (to the NASA-CASA carbon model) on correlations between climate indices with our predicted NEP fluxes has been examined further in a related paper (Potter et al., in review). For example, we find that 15% of total land area shown as having strong correlation of NEP with SOI also shows strong correlation of winter (DJF) PREC with SOI. Just over 34% of total land area shown as having strong correlation of NEP with SOI also shows strong correlation of TEMP with SOI, while only 7% also shows strong correlation of both PREC and TEMP with SOI. We can conclude therefore

that at least 50% of the global land areas shown as having strong correlation of predicted NEP with climate indices results from similarly strong correlations of either PREC and TEMP model inputs with SOI or NAO. The remaining 50% of the global land area shown as having strong NEP correlations must result from FPAR inputs to the NASA-CASA carbon model, which can also correlate significantly with either climate index.

## **5. Concluding Remarks**

Our NASA-CASA model results reveal important patterns of geographic variability in NPP and NEP between and within major continental areas of the terrestrial biosphere. A unique advantage of combining ecosystem modeling with global satellite drivers for vegetation cover properties is to enhance the spatial resolution of sink patterns for CO<sub>2</sub> in the terrestrial biosphere. On the temporal scale, this AVHRR data set used to generate FPAR input to the NASA-CASA model now extends for nearly 20 years of global monthly imagery, which permits model evaluations within the context of other global long-term data sets for climate and atmospheric CO<sub>2</sub> levels. We have begun to identify numerous relatively small-scale patterns throughout the world where terrestrial carbon fluxes may vary between net annual sources and sinks from one year to the next. Predictions of NEP for these areas of high interannual variability will require further validation of carbon model estimates, with focus on both flux algorithm mechanisms and potential scaling errors to the regional level.

**Acknowledgments.** This work was supported by grants from NASA programs in Intelligent Systems and Intelligent Data Understanding, and the NASA Earth Observing System (EOS)

Interdisciplinary Science Program. The NASA-CASA model data sets described in this paper are made available for electronic file transfer from [geo.arc.nasa.gov](http://geo.arc.nasa.gov).

## References

- Behrenfeld, M. J., J. T. Randerson, C. R. McClain, G. C. Feldman, S. Q. Los, C. I. Tucker, P. G. Falkowski, C. B. Field, R. Frouin, W. E. Esaias, D. D. Kolber, and N. H. Pollack, 2001. Biospheric primary production during an ENSO transition. *Science* 291, 2594-2597.
- Bender, M., T. Ellis, P. Tans, R. Francey, and D. Lowe, 1996. Variability in the O<sub>2</sub>/N<sub>2</sub> ratio of southern hemisphere air, 1991-1994: Implications for the carbon cycle. *Global Biogeochem. Cycles*, 10, 9-21.
- Bonan G. B., 1989. A computer model of the solar radiation, soil moisture and soil thermal regimes in boreal forests. *Ecological Modelling*. 45, 275-306.
- Bousquet, P., P. Peylin, P. Ciais, C. Le Quéré, P. Friedlingstein, and P. P. Tans, 2000. Regional changes in carbon dioxide fluxes of land and oceans since 1980 *Science*. 290, 1342-1346.
- Braswell, B. H., D. S. Schimel, E. Linder, and B. Moore, 1997. The response of global terrestrial ecosystems to interannual temperature variability. *Science*, 278, 870-872.
- Buermann, W., J. Dong, X. Zeng, R. B. Myneni, and R. E. Dickinson, 2001. Evaluation of the utility of satellite-based vegetation leaf area index data for climate simulations. *J. Climate*, 14, 3536-3550.
- DeFries R., M. Hansen, and J. Townshend, 1995. Global discrimination of land cover types from metrics derived from AVHRR Pathfinder data. *Remote Sensing of Environment*, 54, 209-222.

- Glantz, M. H., R. W. Katz, and N. Nicholls (eds.), 1991. *Teleconnections linking world-wide climate anomalies*. Cambridge University Press, New York, 527 pp.
- Goetz, S. J., and S. D. Prince, 1998. Variability in light utilization and net primary production in boreal forest stands. *Canadian Journal of Forest Research*. 28: 375-389
- Houghton, R. A., J. L. Hackler, and K. T. Lawrence, 1999. The U.S. carbon budget: contributions from land-use change. *Science*, 285, 574-578.
- Hurrell, J. W., 1995. Decadal trends in the North Atlantic Oscillation regional temperatures and precipitation, *Science*, 269, 676-679.
- IGBP (International Geosphere Biosphere Programme) Terrestrial Carbon Working Group, 1998. The terrestrial carbon cycle: Implications for the Kyoto Protocol. *Science*. 280, 1393-1394.
- Jumikis, A. R., 1966. *Thermal Soil Mechanics*. New Brunswick; Rutgers University Press.
- Keeling, R. F., S. C. Piper, and M. Heimann, 1996. Global and hemispheric CO<sub>2</sub> sinks deduced from changes in atmospheric O<sub>2</sub> concentration. *Nature*, 381, 218-221.
- Kindermann J, G. Würth, and G. H. Kohlmaier, 1996. Interannual variation of carbon exchange fluxes in terrestrial ecosystems. *Global Biogeochem. Cycles*. 10, 737-755.
- Klein, S. A., B. J. Soden, and N-C. Lau, 1999. Remote sea surface temperature variations during ENSO: Evidence for a tropical atmospheric bridge, *J. Climate*, 12, 917-932.
- Knyazikhin, Y., J. V. Martonchik, R. B. Myneni, D. J. Diner, and S. W. Running, 1998. Synergistic algorithm for estimating vegetation canopy leaf area index and fraction of absorbed photosynthetically active radiation from MODIS and MISR data, *J. Geophys. Res.*, 103, 32,257-32,276.

- Maisongrande, P., A. Ruimy G. Dedieu, and B. Saugier, 1995. Monitoring seasonal and interannual variations of gross primary productivity, net primary productivity, and net ecosystem productivity using a diagnostic model and remotely sensed data. *Tellus*, 47B, 178-190.
- Malmström, C. M., M. V. Thompson. G. P. Juday, S. O. Los, J. T. Randerson, and C. B. Field, 1997. Interannual variation in global scale net primary production: Testing model estimates. *Global Biogeochem. Cycles*. 11, 367-392.
- McCabe, G. J., and M. D. Dettinger, 1999. Decadal variations in the strength of ENSO teleconnections with precipitation in the western United States. *Internl. J. Climatol.*, 19, 1399-1410.
- McGuire, A. D., S. Sitch, J. S. Clein, R. Dargaville, G. Esser, J. Foley, M. Heimann, F. Joos, J. Kaplan, D. W. Kicklighter, R. A. Meier, J. M. Melillo, B. Moore III, I. C. Prentice, N. Ramankutty, T. Reichenau, A. Schloss, H. Tian, L. J. Williams, and U. Wittenberg. 2001. Carbon balance of the terrestrial biosphere in the twentieth century: Analyses of CO<sub>2</sub>, climate and land-use effects with four process-based ecosystem models. *Global Biogeochem. Cycles*, 15, 183-206.
- Monteith, J. L., 1972. Solar radiation and productivity in tropical ecosystems. *Journal of Applied Ecology* , 9, 747-766.
- New, M. G., M. Hulme and P. D. Jones, 2000. Representing twentieth-century space-time climate variability. Part II: Development of 1901-1996 monthly grids of terrestrial surface climate. *J. Climate*, 13, 2217-2238.

- Olson, R. J., J. M. O. Scurlock, W. Cramer, W. J. Parton, and S. D. Prince, 1997. *From Sparse Field Observations to a Consistent Global Dataset on Net Primary Production*. IGBP-DIS Working Paper No. 16, IGBP-DIS, Toulouse, France.
- Pacala, S.W., Hurtt, G.C., Baker, D., Peylin, P., Houghton, R.A., Birdsey, R.A., Heath, L., Sundquist, E.T., Stallard, R.F., Ciais, P., Moorcroft, P., Caspersen, J.P., Shevliakova, E., Moore, B., Kohlmaier, G., Holland, E., Gloor, M., Harmon, M.E., Fan, S.-M., Sarmiento, J.L., Goodale, C.L., Schimel, D. and Field, C.B. 2001. Consistent land- and atmosphere-based U.S. carbon sink estimates. *Science*, 292, 2316-2320.
- Parton, W. J., B. McKeown, V. Kirchner, and D., Ojima, 1992. CENTURY Users Manual. Natural Resource Ecology Laboratory. Colorado State University, Fort Collins.
- Potter, C. S., 1999. Terrestrial biomass and the effects of deforestation on the global carbon cycle. *BioScience*. 49, 769-778.
- Potter, C., S. Klooster, M. Steinbach, P. Tan, V. Kumar, S. Shekhar, R. Nemani, R. Myneni, Global teleconnections of climate to terrestrial carbon flux. *J. Geophys. Res.* (In Review).
- Potter, C. S., S. A. Klooster, and V. Brooks, 1999. Interannual variability in terrestrial net primary production: Exploration of trends and controls on regional to global scales, *Ecosystems*. 2, 36-48.
- Potter, C. S., J. T. Randerson, C. B. Field, P. A. Matson, P. M. Vitousek, H. A. Mooney, and S. A. Klooster, 1993. Terrestrial ecosystem production: A process model based on global satellite and surface data, *Global Biogeochem. Cycles.*, 7, 811-841.
- Priestly, C. H. B., and R. J. Taylor, On the assessment of surface heat flux and evaporation using large-scale parameters. *Mont. Weather Rev.* 100:81-92, 1972.

- Rayner, P. J., I. G. Enting, R. J. Francey, and R. Langenfelds. Reconstructing the recent carbon cycle from atmospheric CO<sub>2</sub>, d<sup>13</sup>C, and O<sub>2</sub>/N<sub>2</sub> observations. *Tellus*, 51B, 213-232, 1999.
- Running, S. W, and R. R. Nemani, Relating seasonal patterns of the AVHRR vegetation index to simulated photosynthesis and transpiration of forests in different climates. *Remote Sensing of Environment*. 24, 347-367, 1998.
- Schimel D, House J, Hibbard K, Bousquet P, Ciais P, Peylin P, Apps M, Baker D, Bondeau A, Brasswell R, Canadell J, Churkina G, Cramer W, Denning S, Field C, Friedlingstein P, Goodale C, Heimann M, Houghton RA, Melillo J, Moore III B, Murdiyarso D, Noble I, Pacala S, Prentice C, Raupach M, Rayner P, Scholes B, Steffen W, Wirth C, Recent patterns and mechanisms of carbon exchange by terrestrial ecosystems, *Nature*, 414, 169-172, 2001.
- Sellers, P. J., C. J. Tucker, G. J. Collatz, S. O. Los, C. O. Justice, D. A. Dazlich, and D. A. Randall, A global 1x1 NDVI data set for climate studies. Part 2: the generation of global fields of terrestrial biophysical parameters from the NDVI. *International Journal of Remote Sensing*. 15, 3519-3545, 1994.
- Stockburger, D. W. Introductory Statistics: Concepts, Models, And Applications, WWW Version 1.0, <http://www.psychstat.smsu.edu/sbk00.htm>, 1998,
- Tans, P. P., I. Y. Fung, and T. Takahashi, Observational constraints on the global atmospheric CO<sub>2</sub> budget. *Science*, 247, 1431-1438, 1990.
- Thompson, D. W. J. and J. M. Wallace, 1998. The Arctic Oscillation signature in the wintertime geopotential height and temperature fields, *Geophys. Res. Lett.*, 25, 1297-1300.
- Trenberth, J. W., and K. E. Hurrell, 1994. Decadal atmosphere-ocean variations in the Pacific. *Climate Dynamics*, 9, 303-319.

- USGCRP, 1999. A U. S. Carbon Cycle Science Plan. Report of the Carbon and Climate Working Group, U. S. Global Change Research Program, Sarmiento, J. L. and S. C. Wofsy (eds.), Washington, DC, 69 pp..
- Vuille, M., R. S. Bradley, and F. Keimig, 2000. Climate variability in the Andes of Ecuador and its relation to tropical Pacific and Atlantic sea surface temperature anomalies. *J. Climate*, 13, 2520-2535.
- Vukicevic, T., B. H. Braswell, and D. Schimel, 2001. diagnostic study of temperature controls on global terrestrial carbon exchange. *Tellus*, 53B, 150-170.
- Walker, B., and W. Steffen. 1997. An overview of the implications of global change for natural and managed terrestrial ecosystems. *Conservation Ecology*. 1, 2.
- Walker, G. T. and E. W. Bliss, 1932. World Weather V., *Mem. Roy. Meteor. Soc.*, 4, 53-84.
- Watson, R. T., I. R. Noble, B. Bolin, N. H. Ravindranath, D. J. Verardo and D. J. Dokken (eds). 2000. Land Use, Land-Use Change, and Forestry Special Report of the Intergovernmental Panel on Climate Change. Cambridge University Press, UK. 375 pp.

## Figure captions

Figure 1. Comparison of annual observed NPP to predicted values from the NASA-CASA model (driven by  $0.5^\circ$  FPAR from the satellite AVHRR and climate means from New et al, 2000). The data set of more than 1900 observed NPP points was compiled for the Ecosystem Model-Data Intercomparison (EMDI) activity by the Global Primary Productivity Data Initiative (GPPDI) working groups of the International Geosphere Biosphere Program Data and Information System (IGBP-DIS; Olson et al., 1997).

Figure 2. Schematic representation of components in the NASA-CASA model. The soil profile component [I] is layered with depth into a surface ponded layer ( $M_0$ ), a surface organic layer ( $M_1$ ), a surface organic-mineral layer ( $M_2$ ), and a subsurface mineral layer ( $M_3$ ), showing typical levels of soil water content (shaded) in three general vegetation types. The production and decomposition component [II] shows separate pools for carbon cycling among pools of leaf litter, root litter, woody detritus, microbes, and soil organic matter. Microbial respiration rate is controlled by temperature (TEMP) and litter quality ( $q$ ).

Figure 3. NASA-CASA results from interannual simulations of NEP for North America. (a) monthly predictions, (b) 12 month running mean.

Figure 4. NASA-CASA results from interannual simulations of NEP for Eurasia. (a) monthly predictions, (b) 12 month running mean.

Figure 5. NASA-CASA global NEP results. (a) 12 month running mean, (b) Southern Oscillation Index, 12 month running mean. Both panels reflect a 12-month offset from actual years of model prediction shown in the x-axis.

Figure 6. Predicted interannual variation in annual NEP fluxes for North America, 1986 to 1998.

Figure 7. Smoothed interannual variation in monthly (a) TEMP (12 month running mean), (b) PREC (12 month running sum) for North America, 1982 to 1998.

Figure 8. Locations of co-occurrence between anomalously low (LO) or anomalously high (HI) monthly event observations for climate inputs and NASA-CASA predicted NEP from 1982 to 1998. An anomalous event threshold value was defined as 1.5 standard deviations or greater from the long-term (1982-1998) monthly mean value. Each non-white pixel indicates a location where NEP-LO co-occurs in the time series with (a) PREC-LO or (b) TEMP-LO, and that the color of that pixel indicates the vegetation type at that location.

Figure 1

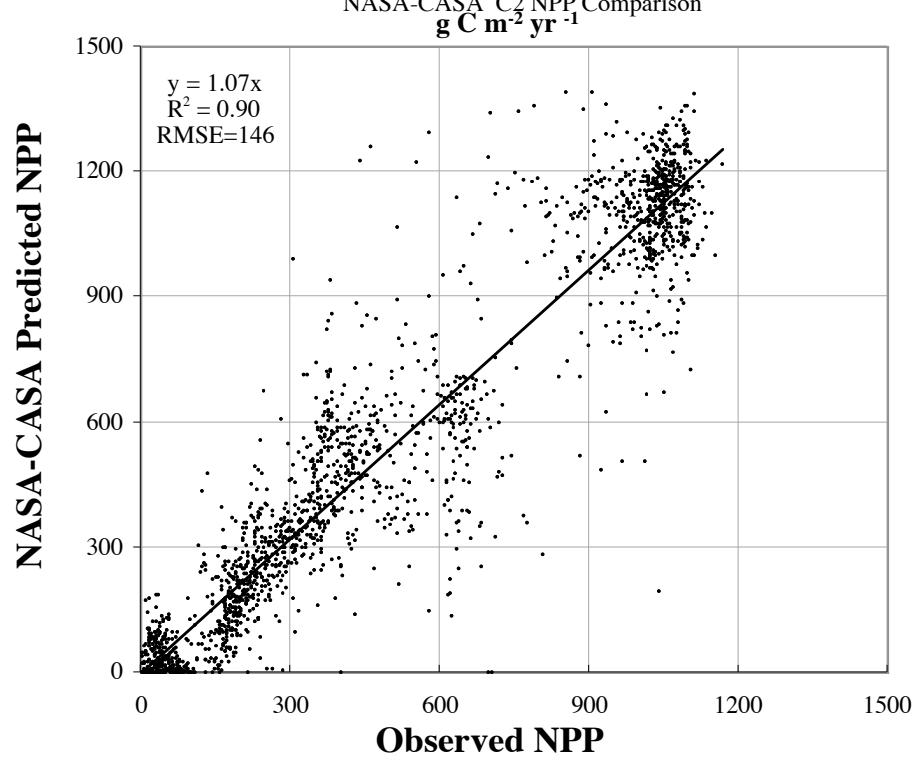


Figure 2

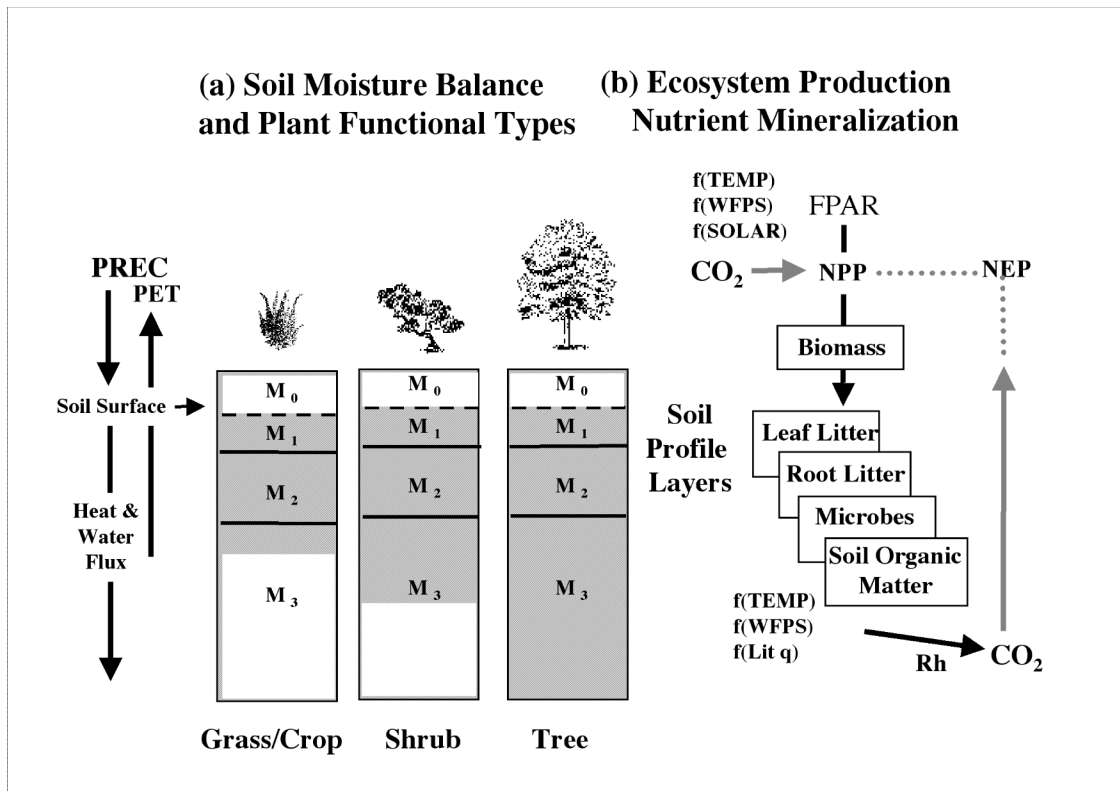


Figure 3

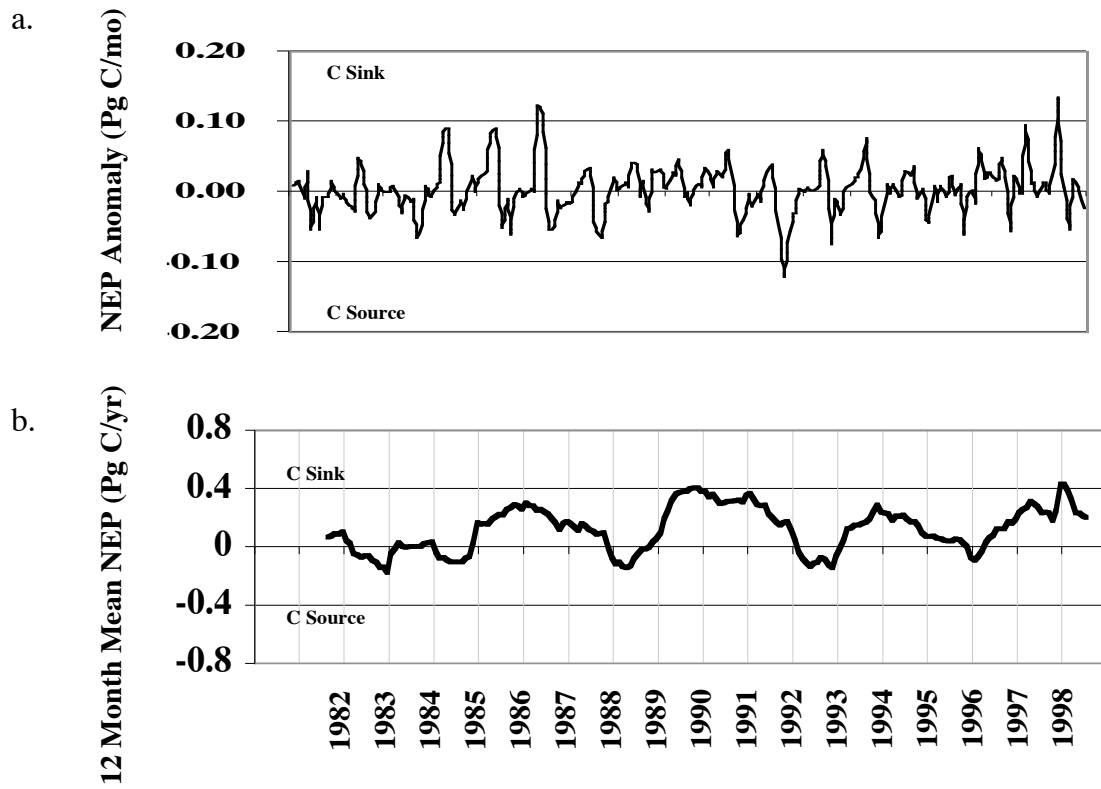
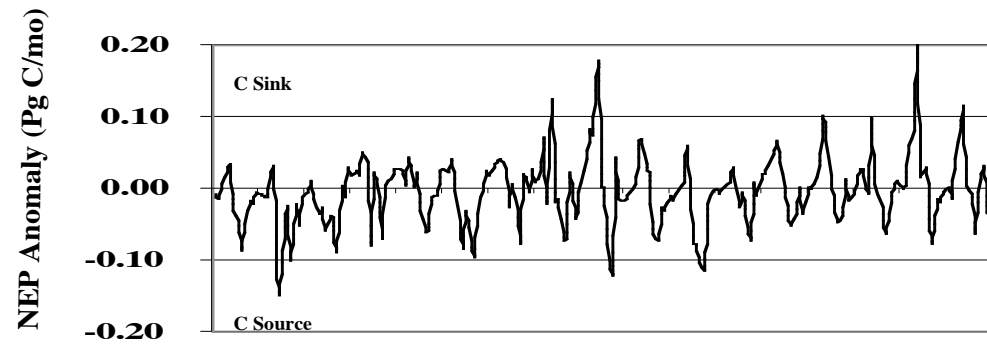


Figure 4

a.



b.

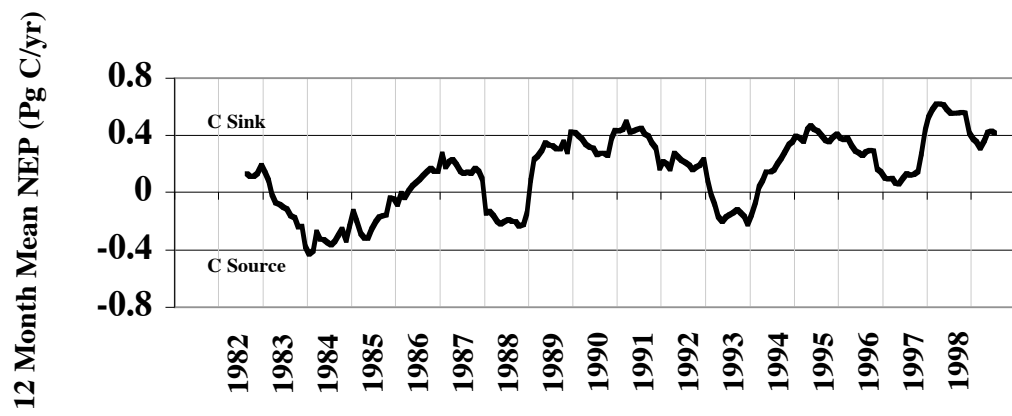


Figure 5

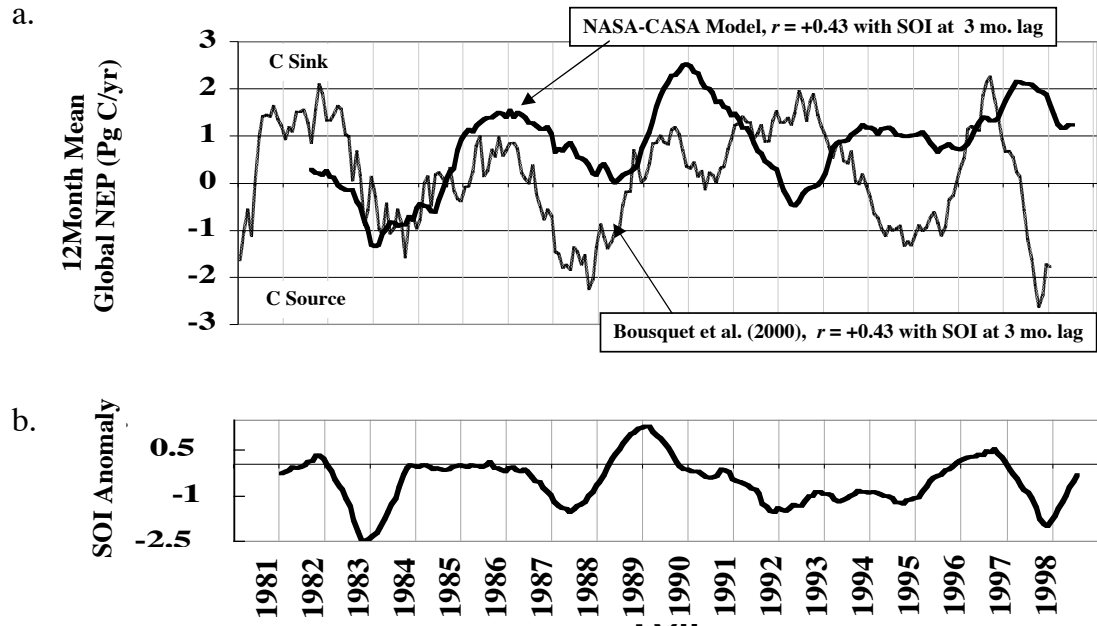


Figure 6

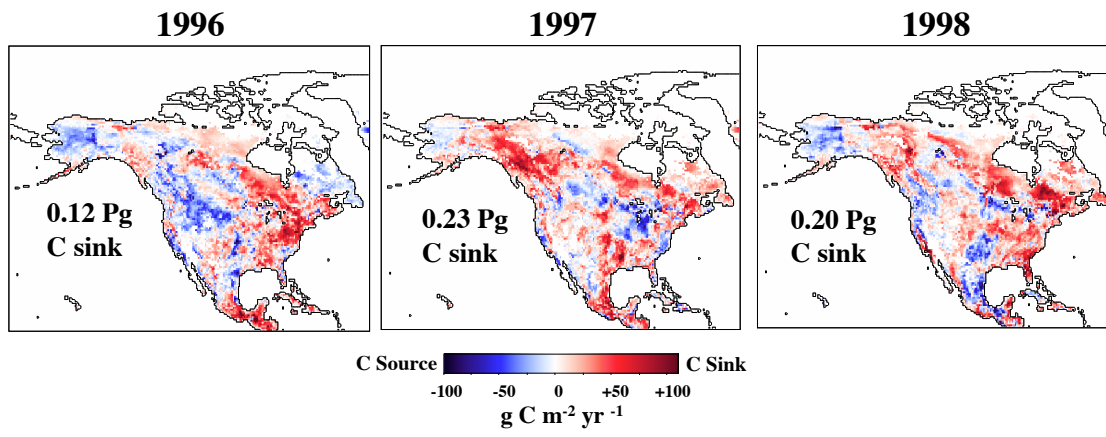
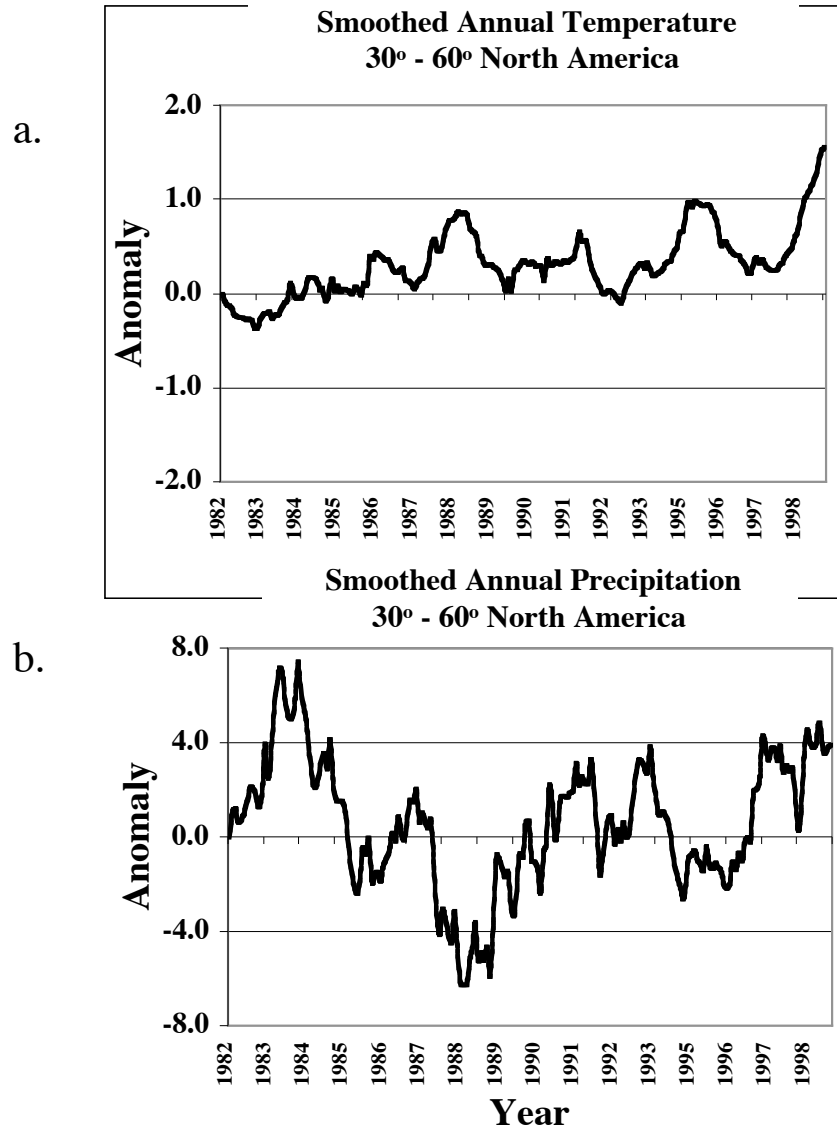


Figure 7



**Figure 8**

